Aerosol deposited in East Antarctica over the last glacial cycle: Detailed apportionment of continental and sea-salt contributions

Matthias Bigler,[1,2] Regine Röthlisberger,[1,3] Fabrice Lambert,[1] Thomas F. Stocker,[1] and Dietmar Wagenbach[4]

Received 6 July 2005; revised 17 November 2005; accepted 13 January 2006; published 28 April 2006.

[1] The major ions, sodium (Na^+), calcium (Ca^{2+}), and chloride (Cl^-), deposited in central Antarctica and preserved in ice cores originate from both marine and continental sources. They provide important proxy records, helping to reconstruct past climatic processes. However, it is difficult to clearly separate the individual contributions from the two sources, particularly the continental one during glacial periods. On the basis of Na^+ and Ca^{2+} records at an unprecedented resolution from the European Project for Ice Coring in Antarctica (EPICA) Dome C ice core back to the penultimate glacial period, mean ion mass ratios were deduced for the continental and the sea-salt aerosol body over East Antarctica. The sea-salt ion mass ratios are in the range predicted for both wind-induced bubble bursting of breaking waves on the open ocean and sea ice brine-derived aerosols, respectively, thus allowing no clear decision on the contribution of sea ice to the central Antarctic sea-salt aerosol. The continental ion mass ratios point to a substantial contribution by halide aerosols, which is in agreement with the source properties in southern South America, although these ratios do not rule out the continental shelf exposed during glacial stages as an additional source. While during cold glacial periods continental sources accounted for more than 90% of the total Ca^{2+} input, this contribution was highly variable during the remaining glacial periods covarying with the Antarctic warm events. During the Holocene it was less than 50%, but it was significantly higher during the last interglacial period. The sea-salt aerosol contribution to the total Na^+ input, which was mostly dominant and higher than 90%, was reduced to only two thirds during the last two glacial maxima and the period around 60 ka. Thus the glacial continental Na^+ contribution appears to be more important than previously assumed, implying that Na^+ records not corrected for continental Na^+ do not represent a pure marine signal at the East Antarctic plateau during glacial times.

Citation: Bigler, M., R. Röthlisberger, F. Lambert, T. F. Stocker, and D. Wagenbach (2006), Aerosol deposited in East Antarctica over the last glacial cycle: Detailed apportionment of continental and sea-salt contributions, *J. Geophys. Res.*, *111*, D08205, doi:10.1029/2005JD006469.

1. Introduction

[2] Ions routinely analyzed in ice cores are related to the water-soluble part of the aerosol and some water-reactive trace gases deposited on glaciers and polar ice sheets. Their depth profiles are preserved in deep ice cores, which bear information on past changes in their long-range transport and in their sources [*Legrand and Mayewski*, 1997; *Ohno et al.*, 2005]. However, because most of the ion species represent a variable mixture of several different sources, the interpretation of chemical ice core records is not straightforward. For example calcium (Ca^{2+}) is commonly used as a proxy for continental aerosol input, however, at remote sites such as East Antarctica its continental present-day contribution is of the same order as the Ca^{2+} fraction originating from the sea-salt aerosol source [*Röthlisberger et al.*, 2002]. Sodium (Na^+) and chloride (Cl^-) on the other hand are generally considered as marine proxies for sea-salt aerosol input. Besides wind-induced bubble bursting of breaking waves on the open ocean, freshly formed sea ice seems to be an important additional source of sea-salt aerosols around Antarctica [*Wagenbach et al.*, 1998; *Wolff et al.*, 2003]. However, some amount of Na^+ and Cl^- is presumably brought in by continental aerosols as well, especially during glacial periods when this input has been relatively large.

[3] The measured ion mass concentrations [Ca^{2+}] and [Na^+] can be separated formally into a sea-salt (shortened to

[1]Climate and Environmental Physics, Physics Institute, University of Bern, Bern, Switzerland.
[2]Now at Ice and Climate Research, Niels Bohr Institute, University of Copenhagen, Copenhagen, Denmark.
[3]British Antarctic Survey, Natural Environment Research Council, Cambridge, UK.
[4]Institut für Umweltphysik, University of Heidelberg, Heidelberg, Germany.

0148-0227/06/2005JD006469$09.00

ss) and a continental (non-sea-salt, shortened to nss) part, given the ion mass ratios of Na^+ and Ca^{2+} of the water-soluble mean continental or non-sea-salt aerosol (hereafter noted as the continental ion mass ratio $(Na^+/Ca^{2+})_{nss}$), and of the mean sea-salt aerosol (hereafter sea-salt ion mass ratio $(Na^+/Ca^{2+})_{ss}$). Note that analogous equations apply for $[Cl^-]$ instead of $[Na^+]$:

$$\left[\mathrm{nssCa}^{2+}\right] = \left[\mathrm{Ca}^{2+}\right] - \left[\mathrm{ssNa}^{+}\right] \cdot \left(\mathrm{Na}^{+}/\mathrm{Ca}^{2+}\right)_{\mathrm{ss}}^{-1} \quad (1)$$

$$\left[\mathrm{ssNa}^{+}\right] = \left[\mathrm{Na}^{+}\right] - \left[\mathrm{nssCa}^{2+}\right] \cdot \left(\mathrm{Na}^{+}/\mathrm{Ca}^{2+}\right)_{\mathrm{nss}} \quad (2)$$

[4] This simple system of linear equations can be solved with respect to $[nssCa^{2+}]$ and $[ssNa^+]$:

$$\left[\mathrm{nssCa}^{2+}\right] = c \cdot \left\{ \left[\mathrm{Ca}^{2+}\right] - \left[\mathrm{Na}^{+}\right] \cdot \left(\mathrm{Na}^{+}/\mathrm{Ca}^{2+}\right)_{\mathrm{ss}}^{-1} \right\} \quad (3)$$

$$\left[\mathrm{ssNa}^{+}\right] = c \left\{ \left[\mathrm{Na}^{+}\right] - \left[\mathrm{Ca}^{2+}\right] \cdot \left(\mathrm{Na}^{+}/\mathrm{Ca}^{2+}\right)_{\mathrm{nss}} \right\} \quad (4)$$

$$\text{with} \quad c = \left[1 - \left(\mathrm{Na}^{+}/\mathrm{Ca}^{2+}\right)_{\mathrm{nss}} \cdot \left(\mathrm{Na}^{+}/\mathrm{Ca}^{2+}\right)_{\mathrm{ss}}^{-1} \right]^{-1} \quad (5)$$

$(Na^+/Ca^{2+})_{ss}$, mainly influential in equation (3), is strongly related to the respective ion mass ratio of bulk seawater. Ratios of the main ions in bulk seawater are well determined and preserved in bubble-bursting-derived sea-salt aerosols. Furthermore, changes over glacial-interglacial periods are assumed to be negligible [*Holland*, 1978]. However, if sea ice formation was involved during the production of sea-salt aerosols, fractionation between different ions occurs and changes the corresponding ratios. For example, in costal Antarctica, sea-salt aerosols produced at low air temperature from brine are significantly depleted in sulfate and to a lesser extent in Na^+ because of mirabilite formation. With respect to Cl^- and Ca^{2+}, both almost not affected by such processes, $[Na^+]$ is shown to be depleted by roughly 10% [*Wagenbach et al.*, 1998], which changes the ion mass ratio $(Cl^-/Na^+)_{ss}$ of 1.8 as found in bulk seawater [*Bowen*, 1979] to 2.0 in brine-derived sea-salt aerosols, whereas $(Na^+/Ca^{2+})_{ss}$ of 26 is changed to approximately 23. However, because $(Na^+/Ca^{2+})_{ss}^{-1}$ is numerically small, the calculation of $[nssCa^{2+}]$ is generally insensitive to such minor changes in the corresponding ratios unless the sea-salt aerosol contribution exceeds the continental one by far.

[5] On the other hand $(Na^+/Ca^{2+})_{nss}$, important in equation (4), relies on the composition of the continental aerosol, which is fairly uncertain, because it depends strongly on the corresponding source material [*Warneck*, 1999] and therefore it needs not to be constant over time. Elemental mass ratios of (Na/Ca), containing both the water-soluble and water-insoluble parts, range from 0.086 for mean sediment, 0.33 for mean soils (with a range over several orders of magnitude) to $(Na/Ca)_{crust} = 0.56$ for mean crust [*Bowen*, 1979]. Moreover, ion mass ratios of the water-soluble part of specific source materials are hardly documented. Therefore the calculation of $[ssNa^+]$ is associated with large uncertainties when the continental aerosol input becomes dominant, as it is the case under glacial conditions.

[6] Since large fractions of the total Ca and almost all Na (and Cl) in central Antarctic ice cores are water soluble [*de Angelis et al.*, 1992; *Ghermandi et al.*, 2003], and the deposition of Ca and Na onto the ice sheet is irreversible (whereas this is usually not the case for Cl [*Röthlisberger et al.*, 2003]; see section 3.4) records of $[nssCa^{2+}]$ and $[ssNa^+]$ serve as proxies for continental and sea-salt aerosol input. However, source separation of $[Ca^{2+}]$ and $[Na^+]$ measurements on Antarctic ice cores has so far been based on literature values of elemental bulk mass ratios of mean crust, often $(Na/Ca)_{crust}$ or $(Na/Al)_{crust}$ [e.g., *de Angelis et al.*, 1987; *Legrand et al.*, 1988; *Röthlisberger et al.*, 2002], although the true ratios could differ significantly from these values. This caused considerable uncertainty, mainly in the resulting $[ssNa^+]$ records.

[7] In this study, we deduce the continental ion mass ratio $(Na^+/Ca^{2+})_{nss}$ and the sea-salt ion mass ratio $(Na^+/Ca^{2+})_{ss}$ directly from high-resolution ice core data gained during the European Project for Ice Coring in Antarctica (EPICA) at Dome Concordia (Dome C). By inspecting the ion mass ratios of individual peaks, we obtain the possible range of these ratios. Events dominated by sea-salt aerosol input will reflect the sea-salt ion mass ratio, whereas major continental events will approach the continental ion mass ratio. As other sources of Ca^{2+} and Na^+ are negligible, the data have to lie within the boundaries set by the sea-salt and the continental ion mass ratios. We assume that peaks do not differ from the rest of the data with regard to the aerosol composition related to respective sources, but that the mix of the two sources within each data point can be highly variable. In addition, on the basis of coarser resolved Cl^- data, the continental ion mass ratios with respect to Cl^- can be deduced and discussed as well.

[8] Our attempt is aimed at a more appropriate apportionment between continental and sea-salt aerosol and temporal changes in the ion mass ratios of the two sources. This sets the stage for upcoming interpretations of the Dome C ice core records in terms of transport and source properties, both related to the southern south hemisphere climate.

2. Data Acquisition and Performance

2.1. Ca^{2+} and Na^+ Data From Dome C

[9] Water-soluble Ca^{2+} and Na^+ have been measured mainly in the field in Dome C during four measuring campaigns between 1997 and 2002 in the frame of EPICA. The remote drill site (75°06′S; 123°21′E) lies 3233 m above sea level and more than 1000 km away from the coasts on the East Antarctic plateau. It is characterized by a mean annual surface temperature of −54.5°C and a low present-day mean accumulation rate of 25 kg m^{-2} a^{-1}, which favors aerosol dry versus wet deposition. The timescale and the accumulation rate estimates are according to *Schwander et al.* [2001] and *EPICA community members* [2004]. The $[Ca^{2+}]$ and $[Na^+]$ records presented by *Röthlisberger et al.* [2004, 2002] are now extended to a depth of 1960 m corresponding to an age of 170 ka. As shown in Figure 1, they cover the Holocene, the last glacial period with its maximum (LGM), the last interglacial (MIS 5e), and partly the penultimate glacial period with its maximum (GM II). Thus data from more than one glacial-interglacial cycle can be examined in detail. In this study we use continuous data

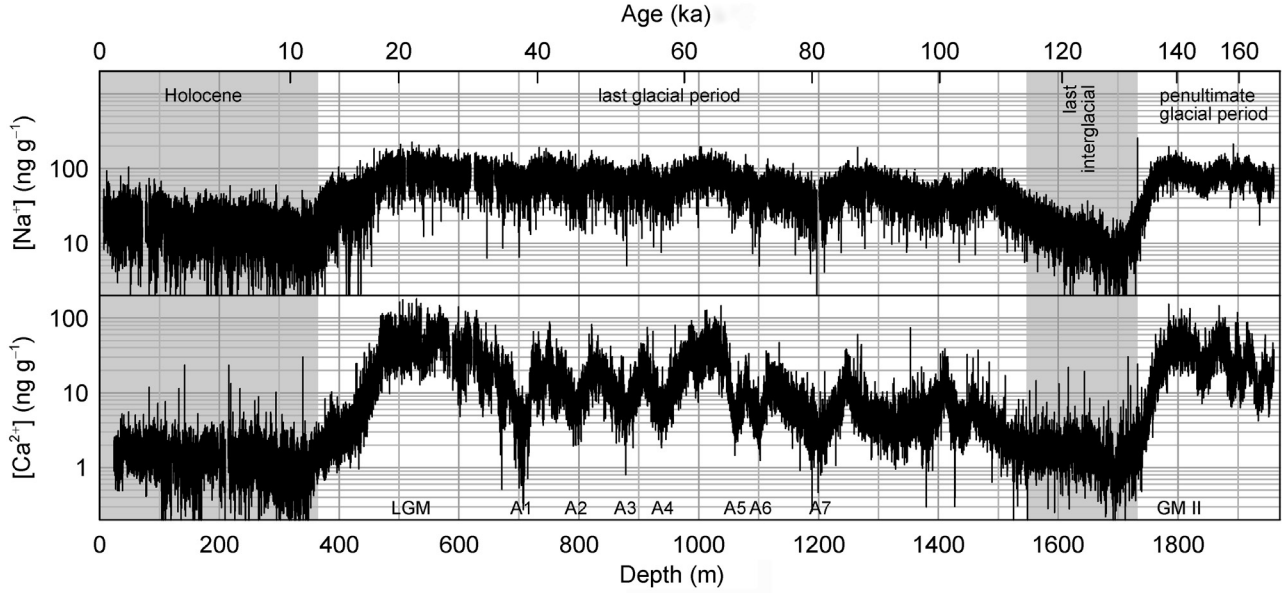

Figure 1. Continuous high-resolution [Ca^{2+}] and [Na^{+}] records (0.5 cm sampling resolution) from the EPICA Dome C ice core covering the time span back to 170 ka on logarithmic *y* axes. The last glacial maximum (LGM), glacial Antarctic warm events A1–A7 [*Blunier and Brook*, 2001], and the maximum of the penultimate glacial period (GM II) are denoted in the lower panel.

with an unprecedented sampling resolution of 0.5 cm (hereafter high-resolution data) giving nearly 400,000 data points for Ca^{2+} and Na^{+} each.

2.2. Performance of the Measurements

[10] For the measurements of Ca^{2+} and Na^{+} we used a continuous flow analysis (CFA) system as described by *Röthlisberger et al.* [2000] based on sensitive fluorescence (for Ca^{2+}) and absorption (for Na^{+}) spectrometric methods performed on continuously longwise melted 1.1 m subsections of the ice core. The measurements were calibrated at regular intervals (one calibration per 3 measured subsections) by measuring standard series for both Ca^{2+} and Na^{+}. Additionally a highly diluted seawater standard (1:10^5) was measured regularly with the Na^{+} detection system resulting in [Na^{+}] = (112 ± 2) ng g^{-1}, which is in good agreement with the expected value of [Na^{+}] = (108 ± 1) ng g^{-1}. Furthermore, our results are in good agreement with IC measurements (linear regression of similar samples of 1.04 for both [Ca^{2+}] and [Na^{+}], with $R^2 = 0.934$ and $R^2 = 0.946$, respectively) [*Littot et al.*, 2002]. The detection limit (defined as three times the standard deviation of blank measurements) is 0.2 ng g^{-1} for [Ca^{2+}], and 3 ng g^{-1} for [Na^{+}], respectively (medians of approximately 150 calibration measurements). Generally the mean measurement errors of [Ca^{2+}] and [Na^{+}] are estimated to be less than ±10% [*Röthlisberger et al.*, 2000]. In the context of this study errors of the concentration of individual peaks in the high-resolution data are rather decisive than mean errors. Therefore they were estimated on the basis of multiple measurements (2 or 3 times) of ice samples from the same depth interval performed on various ice cores. The median of the error of individual peaks is ±7% for [Ca^{2+}] and ±6% for [Na^{+}], respectively. However, true errors of individual peaks might be slightly lower because the variability of multiple measurements was partly caused by real small-scale variations of the concentration value at the same depth.

[11] When determining ion mass ratios on the basis of individual peak values (on which we focus in this study), an additional systematic error might occur because the CFA signal diffusions introduced by small mixing volumes within the measuring setup of Ca^{2+} and Na^{+} (melting device, pump tubes, reaction columns, mixing coils and flow cells) were probably slightly different. To assess this influence, we used a deconvolution approach described by *Rasmussen et al.* [2005], which allowed us to restore the diffused signal at least partly. The restoration filter was based on similar conservative optimum filters for both Ca^{2+} and Na^{+} to account for the signal noise, and on individual mixing filters to account for the slightly different mixing times characterizing the signal diffusions. The exemplary deconvolution of one measurement of LGM ice at a depth of approximately 530 m is shown in Figure 2. We examined $[Na^{+}]/[Ca^{2+}]_{peaks}$ from 12 corresponding peaks. The mean deviation of the ratios from untreated CFA data in comparison with data after applying deconvolution (assumed to be closer to the true values) is +2.5%, which is a reasonably small systematic error compared to the above estimated errors of individual peaks and justifies the use of untreated CFA data for our further systematic analysis.

2.3. Depth Assignment and Depth Resolution Versus Annual Layer Thickness

[12] Mean errors of the depth assignment within the 1.1-m-long samples were estimated by using multiple measurements of ice samples from the same depth interval (as for error estimates of individual peaks in section 2.2). For Ca^{2+} this error is estimated at ±0.4 cm, for Na^{+} at ±0.7 cm. The synchronization of the depth axis of these two components, which are not exactly coregistered because of

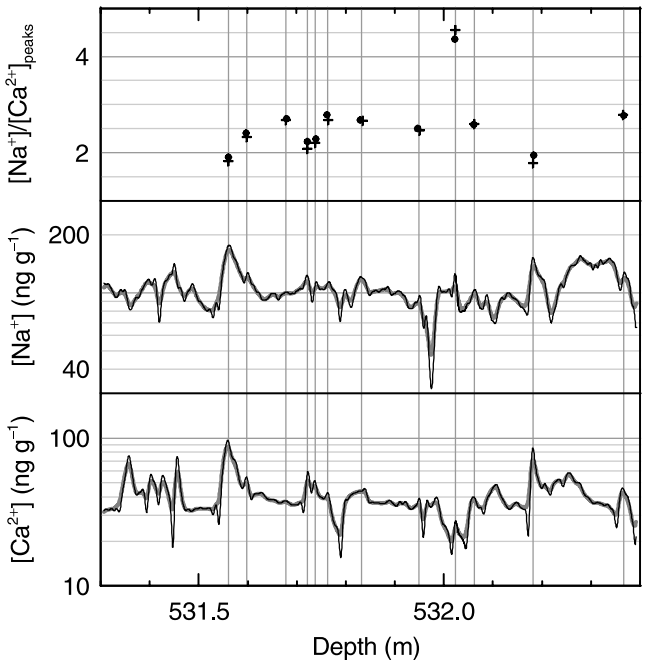

Figure 2. Example of high-resolution [Ca^{2+}] and [Na^{+}] data on logarithmic *y* axes from a LGM sample (gray lines) along with the result of the signal deconvolution (black lines). Ion mass ratios of 12 corresponding peaks show only a small mean deviation when using untreated data (black circles in the uppermost panel) instead of corrected data (black crosses).

the distribution of the meltwater to individual measuring setups, was based on the signal flanks at the beginning and the end of the measurement of each 1.1-m-long sample. The resulting additional error is estimated to be in the same order. Therefore the total error of the depth assignment is around ±1 cm, which has to be considered when calculating ratios between high-resolution Ca^{2+} and Na^{+} data points.

[13] In contrast to the depth assignment the depth resolution of our continuous measurements is more difficult to assess. The question is which depth difference between two layers is necessary to clearly distinguish them or, even more restrictive, to rule out any significant influence between them in terms of the signal amplitude. Two factors are decisive: First, the melting speed of the ice samples, which was 3.9 cm min^{-1} (median) over the whole data set but with 3.5 cm min^{-1} slightly lower during the LGM part and, secondly, the mixing times characterizing the signal diffusions (as mentioned in section 2.2). The latter was estimated most simply by looking at rise (or fall) times of response curves from standard measurements when valves switched from blank water to standard solution (or opposite). The risetime defined as the time required to increase from z% amplitude to $100-z$% amplitude of the reached signal plateau is usually independent from the concentration level c. We assume that one layer in the ice with c_1 is not significantly influenced by its neighboring one with c_2 when we use the measuring uncertainty as the threshold z. Risetimes were found to be around 30 s from measurements of LGM ice and up to 50 s from measurements in deeper ice for Na^{+} but always a few percents lower for Ca^{2+}. Multiplying with the corresponding melting speed leads to a minimum distance between two layers of approximately 1.5 cm in LGM ice and up to 3 cm in deeper ice in order to rule out any significant influence from neighboring layers. The depth resolution in terms of the capability for distinguishing between two events, as used by *Rasmussen et al.* [2005], is approximately half of these values.

[14] Na^{+} data from the penultimate glacial maximum and before show a slightly more smoothed signal compared to Ca^{2+}. This observation might be attributed to postdepositional effects causing diffusion of Na^{+} in older ice despite the fact that *Barnes et al.* [2003] did not find any evidence for such a behavior of Na^{+} in the upper part of the core (above 350 m depth). To avoid larger systematic errors due to postdepositional effects when calculating the ion mass ratios of individual peaks, we used only data from 1715 m depth and above. Down to this depth the calculated mean annual layer thickness hardly ever dropped below 1 cm a^{-1}. Particularly during the last glacial period it remained almost constant around 1.1 cm a^{-1}. However, considering the very low accumulation rate at Dome C and wind driven mixing of the surface snow, seasonal and annual variations are not preserved. Thus our depth resolution, as assessed above, and the chosen sampling resolution of 0.5 cm are sufficient to capture the preserved signal characteristic of Ca^{2+} and Na^{+} in the examined depth interval of the Dome C ice core.

3. Apportionment of Continental and Sea-Salt Ion Mass Ratios

3.1. Examining the High-Resolution Data

[15] To examine the relationship between the high-resolution measurements of [Ca^{2+}] and [Na^{+}], we use a simple scatterplot with logarithmic axes to account for the lognormal distribution of the data. In case of a single aerosol source characterized by a fixed (Na^{+}/Ca^{2+}) ratio, all data points should be aligned along a proportional line given by the (Na^{+}/Ca^{2+}) ratio of the source material. However, such a simple relationship cannot be expected because the contributions of material from a sea-salt and a continental source show different ratios and vary largely. Given the exceptionally high depth resolution of our records and assuming that Ca^{2+} and Na^{+} peaks are not biased by fractionation when coming from the same source, we expect to record occasionally: (1) almost pure sea-salt aerosol input and, (2) under glacial conditions, predominantly continental aerosol input. Both extremes should show up in an upper and lower proportional line limiting the data point scatter and thus representing the continental and sea-salt ion mass ratio, respectively (at the intersections at the argument 1 in the plot). The high-resolution data in Figure 3 (small gray dots) show indeed straight line boundaries: Data from interglacial periods are distinctly limited by a sea-salt ion mass ratio $(Na^{+}/Ca^{2+})_{ss}$, whereas the highest peak values from the last glacial period, for which the continental contribution dominates, lie above a limiting $(Na^{+}/Ca^{2+})_{nss}$ ion mass ratio, both to be deduced in the following subsections. Apart from occasionally predominant sea-salt or continental input, by far most data represent a mixture of the two sources somewhere between the two given boundaries. Another striking limitation of data points from the last glacial period

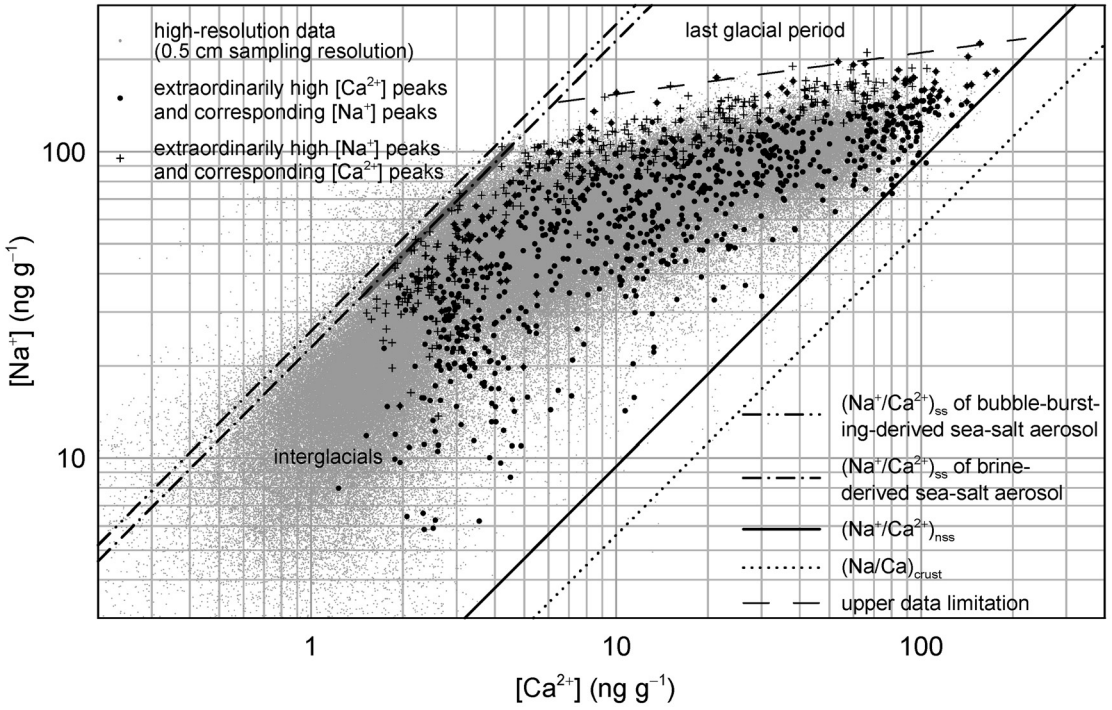

Figure 3. Scatterplot of the high-resolution $[Ca^{2+}]$ and $[Na^{+}]$ data down to 1715 m depth covering the Holocene, the last glacial, and the last interglacial period (small gray dots) on logarithmic axes. Highlighted are exceptionally high peaks (black circles and crosses). See section 3 for detailed discussion of the derived ion mass ratios.

appears as an upper envelope (thin dashed line in Figure 3) and less distinct a lower envelope between the two ion mass ratios. These empirical envelopes determine the maximum and minimum $[ssNa^{+}]$ fractions to the total $[Na^{+}]$ for a given $[Ca^{2+}]$ value and known ion mass ratios.

[16] How can the unknown continental ion mass ratio $(Na^{+}/Ca^{2+})_{nss}$ now be deduced on the basis of our data? Because of the depth assignment uncertainty between the $[Ca^{2+}]$ and the $[Na^{+}]$ records additional errors are introduced when calculating ratios on a point-by-point basis.

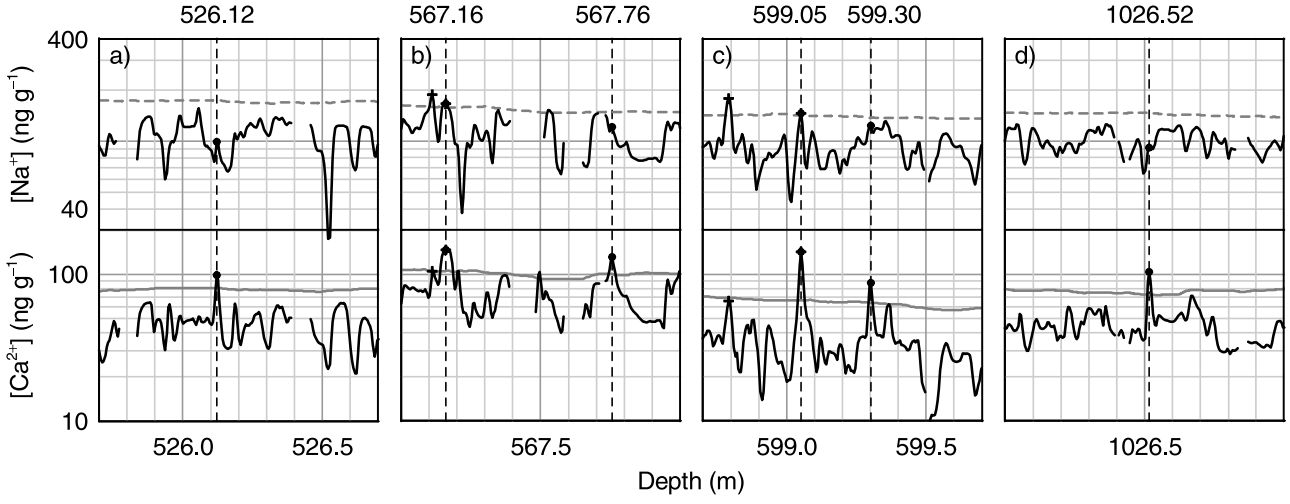

Figure 4. Four exemplary 1 m sections of high-resolution $[Ca^{2+}]$ and $[Na^{+}]$ data (black lines) from the last glacial period (on logarithmic *y* axes), along with the peak criteria used (solid gray lines). Exceptionally high $[Ca^{2+}]$ peaks (black circles in the lower panels) have counterparts (marked with vertical dashed lines) in the $[Na^{+}]$ record (black circles in the upper panels) of different amplitude leading to different values of $[Na^{+}]/[Ca^{2+}]_{peaks}$: (a) 1.01, (b) 1.13 and 0.93, (c) 1.03 and 1.43, and (d) 0.88. Black crosses indicate exceptionally high $[Na^{+}]$ events above the peak criteria (dashed gray line) as discussed in section 3.3.

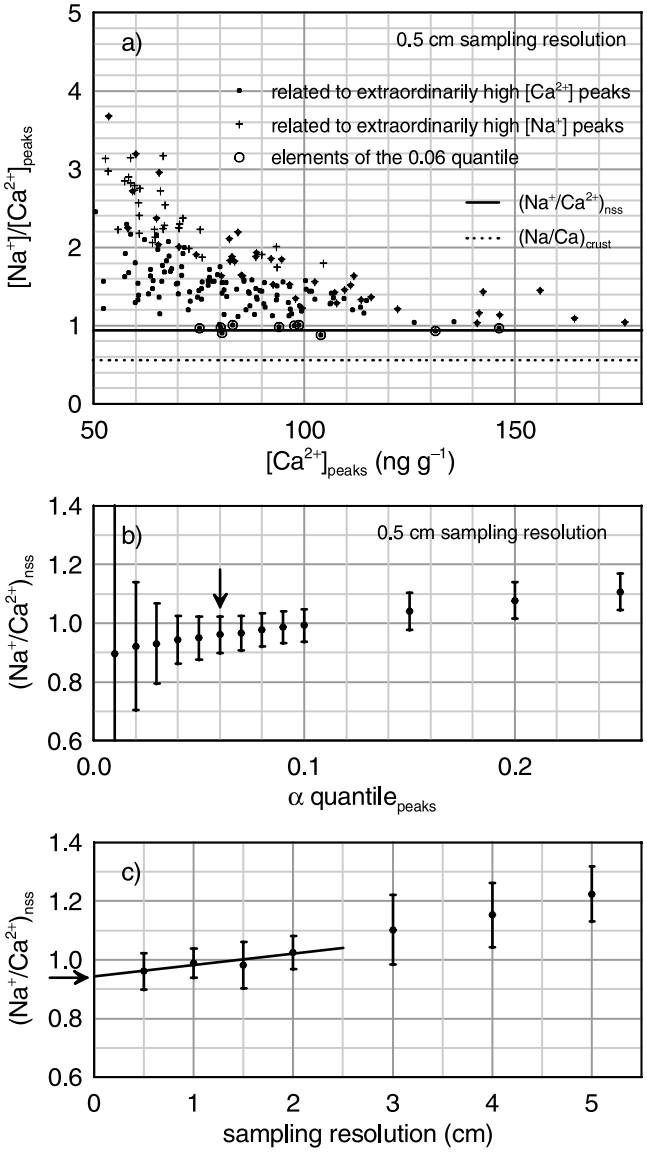

Figure 5. (a) $[Na^+]/[Ca^{2+}]_{peaks}$ of exceptionally high $[Ca^{2+}]$ and corresponding $[Na^+]$ peaks versus $[Ca^{2+}] \geq 50$ ng g^{-1} (solid circles) derived from the high-resolution data. Elements of the 0.06 quantile (marked with open circles) are used to estimate $(Na^+/Ca^{2+})_{nss}$ (solid line), which is clearly higher than $(Na/Ca)_{crust}$ (dotted line). Black crosses indicate exceptionally high $[Na^+]$ events as discussed in section 3.3. (b) Assessment of different α quantiles used to estimate $(Na^+/Ca^{2+})_{nss}$ with the optimal value at $\alpha = 0.06$ (arrow). (c) For sampling resolutions of 2 cm and below (where a convergence behavior is observed) the minor trend can be extrapolated to the intercept, giving $(Na^+/Ca^{2+})_{nss}$ at maximal sampling resolution (arrow).

Especially within peak flanks they are significantly larger than the estimated errors of individual peaks. Therefore the limiting proportional lines (e.g., the ion mass ratios) are not well defined on the basis of all data points (small gray dots in Figure 3). To overcome this problem, we select exceptionally high $[Ca^{2+}]$ peaks to derive the $(Na^+/Ca^{2+})_{nss}$ ratio with the assumption that such peaks are likely to represent mainly continental aerosol input.

3.2. Deducing the Continental Ion Mass Ratio $(Na^+/Ca^{2+})_{nss}$

[17] As a restrictive and robust peak criterion for $[Ca^{2+}]$, we require that the running median of a 2.5 m wide window is exceeded by k times the mean absolute deviation within the same window (using the logarithm of the high-resolution data and $k = 3$). We require furthermore that the $[Ca^{2+}]$ peaks have a corresponding $[Na^+]$ peak within a depth interval of ±0.5 cm to account for the uncertainty in the depth assignment, but without any further restrictions. Examples are shown in Figure 4 and the whole resulting selection of approximately 850 points is added to Figure 3 (black circles). These points spread over the whole range of the high-resolution data indicating that most of them comprise a sea-salt contribution as well. Only a few points, mainly related to very high Ca^{2+} peaks, are lying on a proportional limiting line. Therefore we focus on the approximately 150 points from cold glacial periods ($[Ca^{2+}] > 50$ ng g^{-1}) for which we calculate $[Na^+]/[Ca^{2+}]_{peaks}$. In Figure 5a these ratios are plotted versus $[Ca^{2+}]$, and the convergence to the (now constant) limiting line with increasing $[Ca^{2+}]$ values (from approximately 70 to 180 ng g^{-1}, highlighted with a gray band on the right-hand side in Figure 3) gives evidence (which will be discussed further down) that this line represents $(Na^+/Ca^{2+})_{nss}$.

[18] In order to determine this limiting line, we compare different α quantiles of the selected events. Assuming a normal distribution we calculate the mean value and the standard deviation for each α quantile (weighted with the t distribution, because n is small) and estimate a confidence interval (with 0.1% level of significance) for the $(Na^+/Ca^{2+})_{nss}$ ratio. Figure 5b shows the results with decreasing mean values and increasing confidence intervals for decreasing α quantiles. The minimum of the upper limit of the confidence intervals points to an optimal value of α (arrow in Figure 5b) where possible influences of remaining sea-salt contribution (considering too many points) or analytical errors of individual peaks (considering too few points) are minimal. The corresponding mean value and the confidence interval are a first estimate of $(Na^+/Ca^{2+})_{nss}$ and its error: 0.96 ± 0.06. This result is plotted in Figures 3 and 5a, and it is clearly higher than $(Na/Ca)_{crust}$.

[19] To assess the influence of the sampling resolution on the convergence behavior to the constant limiting line, and therefore on the estimation of $(Na^+/Ca^{2+})_{nss}$, we repeat the same procedure for sampling resolutions between 0.5 and 5 cm (with a constant window width of 2.5 m and a factor k decreasing logarithmically from 3 to 2 to keep the number of selected points approximately constant). We find that for a sampling resolution above 2 cm the convergence behavior disappears. However, resolutions of 2 cm and better show only a minor trend toward a smaller $(Na^+/Ca^{2+})_{nss}$ ratio as indicated in Figure 5c. Extrapolation to the intercept (maximal sampling resolution) by weighted linear regression results in $(Na^+/Ca^{2+})_{nss} = 0.94 \pm 0.07$ (see also Table 1).

[20] As mentioned above the observed convergence of $[Na^+]/[Ca^{2+}]_{peaks}$ to a constant limiting line for increasing $[Ca^{2+}]$ values gives evidence that almost pure continental aerosol input is recorded in the Dome C ice core on a few exceptional occasions. Otherwise the observed limiting constant line would yield strange limitations to

Table 1. Continental and Sea-Salt Ion Mass Ratios

Ion Mass Ratio	Range[a]
Continental Ion Mass Ratios	
$(Na^+/Ca^{2+})_{nss}$	0.87–1.01
$(Cl^-/Ca^{2+})_{nss}$	0.8–1.7[b]
$(Cl^-/Na^+)_{nss}$	0.9–1.8[b]
Sea-Salt Ion Mass Ratios	
$(Na^+/Ca^{2+})_{ss}$	22–26[b]
$(Cl^-/Ca^{2+})_{ss}$	47
$(Cl^-/Na^+)_{ss}$	1.8–2.0[c]

[a]Including both error estimates and the range given by the possible influence of bubble-bursting-derived or brine-derived sea-salt aerosols.
[b]Lower values correspond to brine-derived sea-salt aerosols, upper values to bulk seawater or bubble-bursting-derived sea-salt aerosols.
[c]Vice versa compared to footnote b.

the $[ssNa^+]/[Na^+]$ and the $[nssCa^{2+}]/[Ca^{2+}]$ fraction: Assuming $(Na/Ca)_{crust} = 0.56$ (instead of our deduced value for $(Na^+/Ca^{2+})_{nss}$), $(Na^+/Ca^{2+})_{ss} = 26$ and the empirical envelope $[Na^+] \leq 113 \cdot [Ca^{2+}]^{0.135}$ (thin dashed line at the top of Figure 3) we would get for 70 ng $g^{-1} \leq [Ca^{2+}] \leq 180$ ng g^{-1} an increasing minimal $[nssCa^{2+}]/[Ca^{2+}]$ fraction from 91% to 97% whereas the maximal fraction remains constant on 98.5%. Such a narrow restriction not extended to 100% is unlikely. In parallel the maximal $[ssNa^+]/[Na^+]$ fraction would decrease from 82% to 57% while the minimal one is constant at 41%. With our proposed $(Na^+/Ca^{2+})_{nss}$ ratio on the other hand $[nssCa^{2+}]/[Ca^{2+}]$ reaches 100% and $[ssNa^+]/[Na^+]$ 0% at least for a few aerosol deposition events in Dome C during the last glacial period.

3.3. Inspecting the Sea-Salt Ion Mass Ratio $(Na^+/Ca^{2+})_{ss}$

[21] Assuming that high $[Na^+]$ peaks mainly represent sea-salt aerosol input a similar approach is applied to check whether the sea-salt ion mass ratio derived by our high-resolution data agrees with the expected value. We select exceptionally high $[Na^+]$ peaks of the whole record and the corresponding $[Ca^{2+}]$ peaks (similar as in section 3.2). The resulting selection is shown in Figures 3, 4, and 5a as black crosses. Some $[Na^+]$ peaks are coinciding with the exceptionally high $[Ca^{2+}]$ peaks (when both exceeding the peak criterion). A convergence to a proportional limiting line is found for high $[Na^+]$ values in the range between 40 and 110 ng g^{-1} from interglacial and warmer glacial periods (left gray band in Figure 3) whereas values related to colder glacial conditions snap off from this line because they are influenced by increased admixture of continental aerosols. However, high $[Na^+]$ peaks are always close to the top left margin of the possible range of all data points. To deduce $(Na^+/Ca^{2+})_{ss}$, we focus therefore on events with $[Ca^{2+}] <$ 6.3 ng g^{-1} and we find $(Na^+/Ca^{2+})_{ss} = 23 \pm 1$ (Figure 6), which is slightly lower than the ion mass ratio in bubble-bursting-derived sea-salt aerosol of 26, but corresponds to brine-derived sea-salt aerosols with a value of 23 (see section 1).

[22] A separation of the contribution of bubble-bursting-derived and brine-derived sea-salt aerosol is not possible on the basis of our data because of the only small difference between these two ratios and because of an increasing influence of continental aerosol input during colder glacial periods (see section 4.1). However, our result still gives some evidence that brines related to sea ice formation act as a significant source of Na^+, not only at Antarctic coastal, but also at inland sites as Dome C, at least for events with an exceptionally high $[Na^+]$ input during interglacial and warmer glacial periods. Occasional input of brine-derived sea-salt aerosol at inland sites have been reported recently by *Hara et al.* [2004] and *Wolff et al.* [2003]. The importance of brines on sea ice as Na^+ source may be even higher during colder glacial periods. However, our attempt based on ratios of exceptionally high peaks probably favors brine-derived versus bubble-bursting-derived sea-salt aerosol input events considering the seasonality of the mean Na^+ input, which is presently peaking in winter or spring [*Göktas et al.*, 2002; *Sommer et al.*, 2000], when brine-derived aerosols are likely most influential. Some of the sea-salt aerosol input which is not related to exceptionally high Na^+ peaks may still result from bubble bursting over the open ocean as reported from measurements over recent time periods [e.g., *Fischer et al.*, 2004; *Hara et al.*, 2004]. As a consequence our assumption that high Na^+ represents mainly sea-salt aerosol input is correct for brine-derived, but not for open-water-derived sea-salt aerosol. Thus we cannot pin down the exact sea-salt ion mass ratio $(Na^+/Ca^{2+})_{ss}$ in Dome C, but it is very likely in the range between 22 and 26 (Table 1). This does not exclude sea ice to exert an overall control on the sea-salt aerosol production. However, in contrast to the calculation of ratios with respect to Cl^-, using any sea-salt ion mass ratio in this range does not affect the calculation of $nssCa^{2+}$ and $ssNa^+$ very much.

3.4. Calculating Continental Ion Mass Ratios With Respect to Cl^-

[23] Analogous to $[ssNa^+]$ (equation (2)), $[ssCl^-]$ can be calculated on the basis of $[Cl^-]$ and $(Cl^-/Ca^{2+})_{nss}$, whereas $[nssCa^{2+}]$ (equation (1)) can be expressed on the basis of $[Ca^{2+}]$, $[ssCl^-]$ and $(Cl^-/Ca^{2+})_{ss}$ giving four equations altogether. With $[Ca^{2+}]$, $[Na^+]$ and additionally $[Cl^-]$ [*Röthlisberger et al.*, 2003], $(Na^+/Ca^{2+})_{nss} = 0.94$ (this study), $(Na^+/Ca^{2+})_{ss} = 23–26$ (this study), and $(Cl^-/Ca^{2+})_{ss} = 47$ (almost not affected by fractionation; see section 1) we calculate continental ion mass ratios of $(Cl^-/Ca^{2+})_{nss}$ and $(Cl^-/Na^+)_{nss}$, respectively, although based on a much coarser resolution. Because of significant postdepositional mobilization of Cl^- at Dome C, only samples with high $[Ca^{2+}]$ are considered, where postdepositional effects are minor

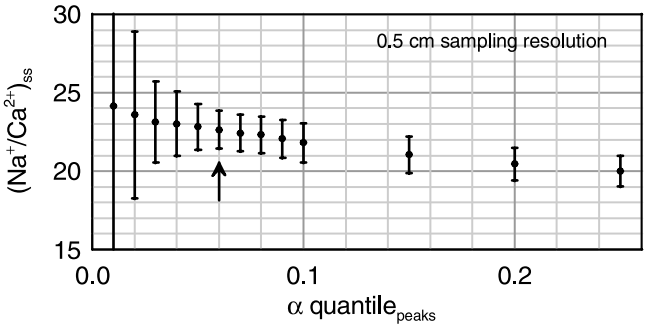

Figure 6. The α quantiles of $[Na^+]/[Ca^{2+}]_{peaks}$ calculated from exceptionally high $[Na^+]$ peaks and corresponding $[Ca^{2+}]$ peaks from interglacial periods. Optimal value at $\alpha = 0.06$ (arrow).

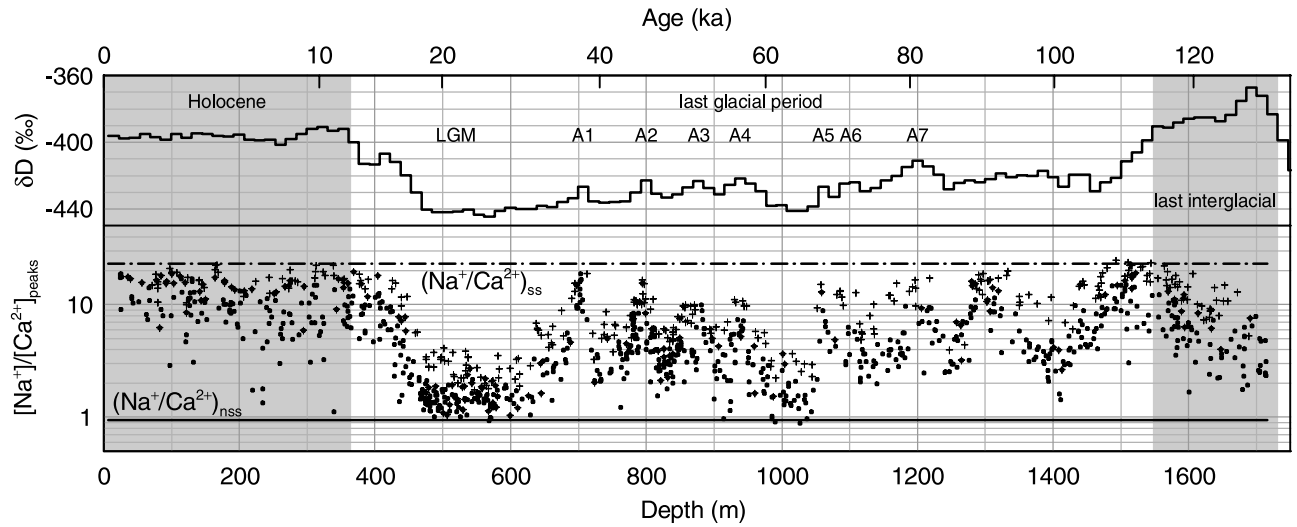

Figure 7. $[Na^+]/[Ca^{2+}]_{peaks}$ values of exceptionally high $[Ca^{2+}]$ and corresponding $[Na^+]$ peaks (black circles) and vice versa (black crosses) versus depth, together with the derived continental ion mass ratio $(Na^+/Ca^{2+})_{nss}$ (solid black line) and the sea-salt ion mass ratio $(Na^+/Ca^{2+})_{ss}$ (dash-dotted line). In the upper panel, δD is shown to give an indication of climatic stages [*EPICA community members*, 2004].

[*Röthlisberger et al.*, 2003]. We used only data from the last glacial maximum within the depth interval from 465 to 612 m. The resulting ratios are $(Cl^-/Ca^{2+})_{nss} = 1.1-1.5$ and $(Cl^-/Na^+)_{nss} = 1.2-1.6$ (with an error for both ratios of ±0.3 for the lower and ±0.2 for the upper value, considering the mentioned errors of the input values; Table 1). Thus we find approximately 30% lower values, if the sea-salt aerosol originates from brine instead of bubble-bursting-derived aerosols.

4. Discussion and Implications

[24] We evaluated Ca^{2+}, Na^+ and Cl^- data in detail with regard to mean ion mass ratios in the water-soluble continental aerosol reaching the EPICA Dome C site and we found that $(Na^+/Ca^{2+})_{nss}$ is close to 1 or somewhat less, and that $(Cl^-/Na^+)_{nss}$ or $(Cl^-/Ca^{2+})_{nss}$ resemble more sea-salt than continental ion mass ratios (Table 1). These findings are mainly based on data from colder glacial periods and should thus be regarded representative for the maximum continental aerosol inputs. On the other hand we find during the interglacial and warmer glacial periods, an ion mass ratio in the sea-salt aerosol $(Na^+/Ca^{2+})_{ss}$ close to or slightly below the expected ratio (Table 1). In the following, our data-deduced ion mass ratios are discussed in terms of their temporal change, aerosol characteristics, most probable source apportionment, and importance of the transport from the continental source area to East Antarctica. This includes as well the respective contributions of the sea-salt and the continental source, apparent preservation of the bulk seawater ratio during the dusty LGM, and the systematic uncertainties when calculating elemental enrichment factors on the basis of ion data sets derived from such ice cores.

4.1. Temporal Dependence of the Ion Mass Ratios

[25] The temporal dependence of the derived continental $(Na^+/Ca^{2+})_{nss}$ and sea-salt $(Na^+/Ca^{2+})_{ss}$ ion mass ratios is shown in Figure 7, where all the $[Na^+]/[Ca^{2+}]_{peaks}$ values as shown in Figure 3 are plotted versus depth. $(Na^+/Ca^{2+})_{ss}$ is expected to be almost constant over the last glacial-interglacial cycle and probably further back. Indeed, peak ratios close to $(Na^+/Ca^{2+})_{ss}$ are found throughout the whole Holocene and the late last interglacial period, but also in the first half of the last glacial period and during the glacial warm events A1 and A2. Only during the LGM and around 60 ka, where the continental aerosol input masks the sea-salt contribution, no peak ratios close to $(Na^+/Ca^{2+})_{ss}$ are found. Interestingly, $(Na^+/Ca^{2+})_{ss}$ is reached only in the later part of the last interglacial period (MIS 5e), with consistently lower values before. This points to considerable differences between MIS 5e and the Holocene interglacials as related to the relatively lower $[Na^+]$ and higher $[Ca^{2+}]$ levels in MIS 5e compared to the Holocene.

[26] The assumption that the continental aerosol ratio $(Na^+/Ca^{2+})_{nss}$ remained constant over time (being independent from long-term climate change) would not hold true if the change in the continental dust source strengths [*Röthlisberger et al.*, 2002] went along with a change in the continental source mix (e.g., via perturbations of the hydrological cycle). Our deduction of $(Na^+/Ca^{2+})_{nss}$ relies on $[Na^+]/[Ca^{2+}]_{peaks}$ values from the LGM and from around 60 ka, but values close to $(Na^+/Ca^{2+})_{nss}$ are found sporadically also during the remaining part of the last glacial period and even during the Holocene and MIS 5e, respectively (Figure 7). This may indicate that only moderate changes in the continental source mix occurred over these time periods.

4.2. Comparison With Characteristic Source Materials

[27] A $(Cl^-/Na^+)_{nss}$ in the range between 0.9 and 1.8 (Table 1) as derived from Dome C LGM data is much higher than elemental ratios (Cl/Na) in mean crust (0.0057), mean soil (0.02, with a range over several orders of magnitude) or mean sediment (0.033). It is closer to the elemental ratio of 2.0 in marine clay [*Bowen*, 1979], thus resembling more a marine than a continental ratio. Relatively high (Cl^-/Na^+) values (along with a strong covariance among Cl^-, Na^+ and Ca^{2+}) are also observed in

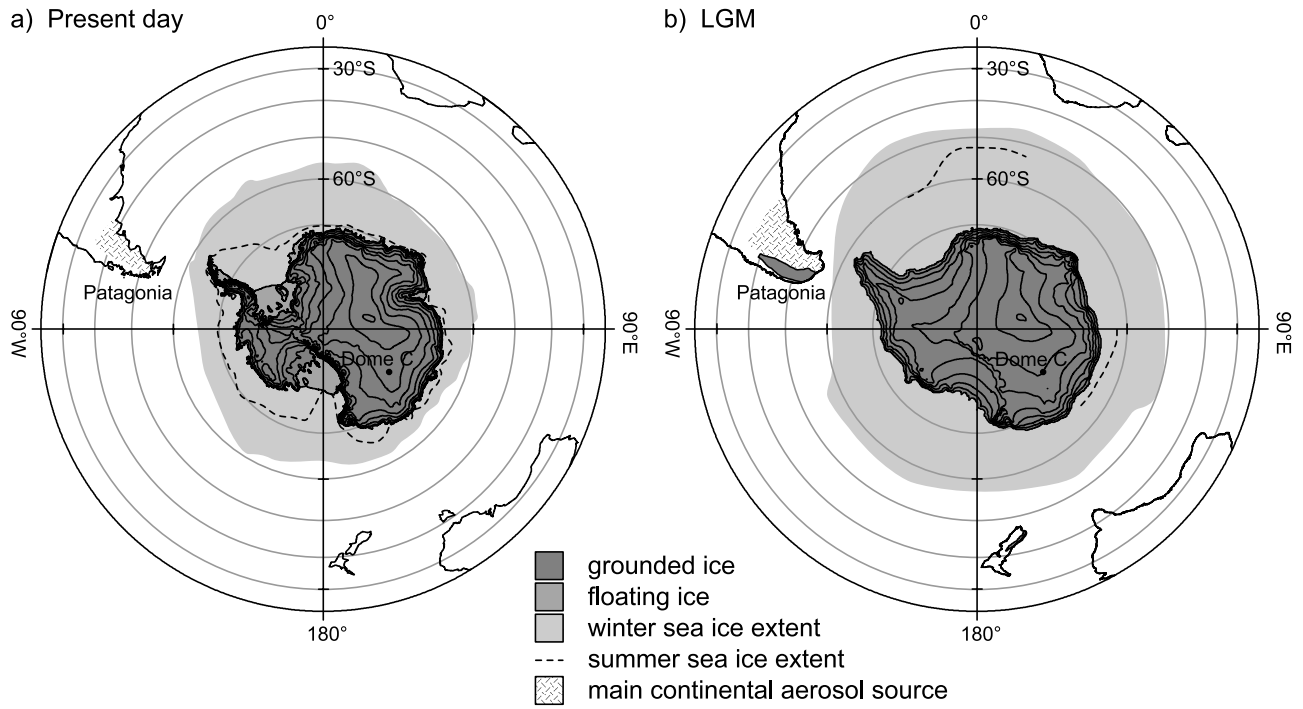

Figure 8. Antarctica (with Dome C) and the surrounding Southern Hemisphere for (a) present-day and (b) LGM. Ice sheets (with 500 m height contour lines) and coastlines are according to *Huybrechts and Zweck* [2006], and winter and summer sea ice extents are from *Gersonde et al.* [2005]. The potential southern South American source region of continental aerosol (see section 4.3) transported to Dome C is hatched.

midlatitude cold glaciers at various high-altitude mountain drill sites which are subject to large continental aerosol input (e.g., European Alps with 1.5 in summer layers [*Legrand et al.*, 2002], Siberian Altai with a value of 1.5 [*Olivier et al.*, 2003], central Tien Shan, northwest China with 1.2 [*Kreutz et al.*, 2001], and other sites [*Wake et al.*, 1993]). Considering the relatively small influence of sea-salt aerosol at these sites, this suggests a significant contribution of halides, mobilized from continental evaporate deposits, which may support the high $(Cl^-/Na^+)_{nss}$ ratio seen in Dome C as well.

[28] Similarly our $(Na^+/Ca^{2+})_{nss} = 0.94 \pm 0.07$ (Table 1) exceeds the elemental mass ratios of (Na/Ca) in mean sediment (0.086), mean soils (0.33, with a range over several orders of magnitude) and in mean crust (0.56). Again the marine clay ratio of 1.1 [*Bowen*, 1979] comes much closer to our value. However, this appears less consistent with current observations at the continental midlatitude sites mentioned above, where the $(Na^+/Ca^{2+})_{nss}$ ratios are clearly lower: *Legrand et al.* [2002] find 0.16 in average summer layers and 0.071 in Sahara dust layers, whereas *Olivier et al.* [2003] report approximately 0.12, and *Kreutz et al.* [2001] report approximately 0.19. Although difficult to assess, the elemental mass ratio (Na/Ca) of continental aerosol deposits at Illimani ice core in the eastern Bolivian Andes is 0.98 within 80 years of dry seasons [*Correia et al.*, 2003], again pointing to a substantial contribution of continental halides at this particular site.

[29] In summary our continental ion mass ratios point to a significant contribution of marine clays and/or halides (as mobilized from continental evaporate deposits). However, in view of the large spatial variability in the ion mass ratios at continental sites a further validation of the Dome C ratios should be relied on the assumed source areas of the continental aerosol deposited in East Antarctica.

4.3. Comparison With Continental Aerosols From the Potential Source Region

[30] Isotopic fingerprints measured on mineral dust in Antarctic ice core samples restrict the possible source areas during glacial periods mainly to southern South America. The provenance remained almost unchanged over different glacial stages, despite the observed huge dust concentration variations [*Basile et al.*, 1997; *Delmonte et al.*, 2004; *Grousset et al.*, 1992]. *Smith et al.* [2003] restrict the glacial continental aerosol source even more to regions south of 37°S, (Figure 8) thus the southern Pampas and Patagonia, the only landmass of significant size in the Southern Hemisphere located inside the Westerlies. This wind system is believed to control local climate by discharging most of the water content over the Andes and continuing as dry winds to the east producing an orographically induced desert [*Iriondo*, 2000]. Aridity, vegetation cover, high wind speeds, and chemical and physical weathering are important factors to produce continental aerosols. However, the persistent availability of potential material to produce continental aerosols is a more important factor than the actual extent of the arid region itself [*Leinen and Sarnthein*, 1987; *Prospero et al.*, 2002].

[31] *Bowen* [1979] finds that the highly mobile ions Cl^- and Na^+ are generally expected to be depleted at the surface of soils where rainfall is abundant but enriched at the

surface of arid soil as they appear in the debated source region. Unfortunately, continental ion mass ratios of southern South American glacial aerosols are hardly documented, but assuming that the ion composition in the source region did not change much, we compare our results from Dome C to present-day properties of the aerosol and soils in the southern Pampas and Patagonia. *Ramsperger et al.* [1998a, 1998b] examined windblown dust at four different sites around 38°S (three of them not influenced by sea-salt aerosols, on which we focus here) at monthly resolution over three years. The mineralogical composition of soils and aeolian dust at these sites were quite uniform over the observation period, suggesting a constant dust source. The dust and soil samples show distinctly higher halide concentrations compared to average West African dust, for example. (Na^+/Ca^{2+}) of water-soluble ions in windblown dust was found to be close to 1, and (Cl^-/Na^+) close to 2, both in agreement with our results. When looking at ion mass ratios in soil instead of air-blown dust, even higher enrichments of Na^+ and Cl^- are found [*Bouza et al.*, 1993; *Ramsperger et al.*, 1998a, 1998b]. Also, *Prospero et al.* [2002] point to the fact that these arid and subarid areas contain vast saline areas.

[32] The role of the exposed continental shelf around southern South America (Figure 8) as a dust source during glacial periods is discussed controversially. *Basile et al.* [1997] rule out a significant contribution on the basis of a few isotopic measurements, whereas *de Angelis et al.* [1992] and *Delmas and Petit* [1994] conclude that the continental shelf was the dominant source during glacial periods providing a mixture of marine clays, carbonate and sea salt, on the basis of examinations of the chemical composition of Antarctic ice core samples. To overcome the problem of a similar ion composition of present-day aerosol in Antarctica although the continental shelf is no potential source any more, *Delmas and Petit* [1994] speculate that the present-day dust originates from aeolian deposits in southern South America that accumulated on the continent during glacial periods from material of the continental shelf. By contrast, *Zárate* [2003] pointed to outwash plains from the Patagonian fluvial system probably formed on the emerged continental shelf with high sediment abundance. In this case the continental shelf served rather as a platform to provide continental aerosols produced by fluvial and cryogenic processes, than as an independent source. In either case, one would expect an imprint of the sea level rise in the continental aerosol record from Dome C during glacial terminations. Indeed, the decrease in Ca^{2+} from LGM to Holocene values happens at the same time as the gradual sea level rise between 17 and 8 ka. However, a small rapid sea level rise around 14 ka, which is seen in marine sedimentary deposits from the Argentine shelf [*Guilderson et al.*, 2000], coincides with a period of almost no changes in continental aerosol input at Dome C [*Röthlisberger et al.*, 2002].

[33] In summary, the composition of the continental aerosol at Dome C is consistent on the one hand with halide continental aerosol from Patagonia or the southern Pampas, and on the other hand with marine clays probably originating directly or indirectly from exposed continental shelf areas. Thus the influence of the exposed shelf areas cannot be ruled out. However, the existence of halide continental aerosols was insufficiently considered so far.

4.4. Transport of Continental Aerosol to Dome C

[34] To assess whether it is reasonable to expect on very few occasions chemically almost unaltered continental aerosol input at Dome C on an event base, the spiral-shaped westward transport from the source region in southern South America to the East Antarctic plateau and the potential degree of scavenging by precipitation have to be considered. Current model results of transport under glacial conditions show inconsistent results. While *Lunt and Valdes* [2001] find a lower transport efficiency and small interannual variations during the LGM compared to present-day (on the basis of analysis of back trajectories initialized in Dome C), *Krinner and Genthon* [2003] conclude that the dust transport to Dome C was slightly faster during the LGM (on the basis of GCM simulations). However, in general interglacial-glacial changes in the aerosol transport to Dome C are considered to be small compared to changes in the source region [*Röthlisberger et al.*, 2002]. Qualitatively, this is supported by the quite similar topographic conditions, i.e., extent and shape of the Antarctic ice sheet [*Huybrechts and Zweck*, 2006] during LGM and present-day (Figure 8).

[35] However the maximum sea ice extent (i.e., winter sea ice) reached much further north during LGM in the sector where continental aerosols are transported from the source to Dome C [*Gersonde et al.*, 2005] (Figure 8). It is conceivable that years with exceptionally large winter sea ice extent were more frequent during maximum glacial periods than during interglacial periods, and that such years were potentially associated with exceptionally large perennial sea ice. During such years, little or no sea-salt aerosol should have mixed with the continental aerosol reaching Dome C, as the contribution from open water must have been minimal because of the extent of the winter sea ice, and the contribution from sea ice is expected to be small because perennial sea ice is not a significant source of sea-salt aerosol [*Wolff et al.*, 2003]. Note that our data-deduced continental ion mass ratio is based on such extremely rare events and that the continental and sea-salt aerosol are usually intimately mixed when deposited in Dome C.

[36] During interglacial periods, conditions that almost completely prevent a substantial mixture of sea-salt and continental aerosol are less likely. Apart from the generally much lower dust to sea-salt ratio during these periods also the sea ice extent was reduced (Figure 8) and the probability for large areas of perennial sea ice much lower. Nevertheless, there are many present-day analogs of prominent transcontinental dust storms that deposit continental aerosols thousands of kilometers away from their sources as from Africa and east Asia [*Harrison et al.*, 2001; *Prospero et al.*, 2002]. Such dust plumes are even known to penetrate far into the Arctic episodically [*Bory et al.*, 2003; *Sun*, 2002]. However, no clear indication can be obtained as to whether they may pick up substantial amounts of sea salt en route, since halides are known to be included in the dust plumes already from the continental source regions. Furthermore, these prominent long-range transport events, mainly reported from the Northern Hemisphere, can hardly

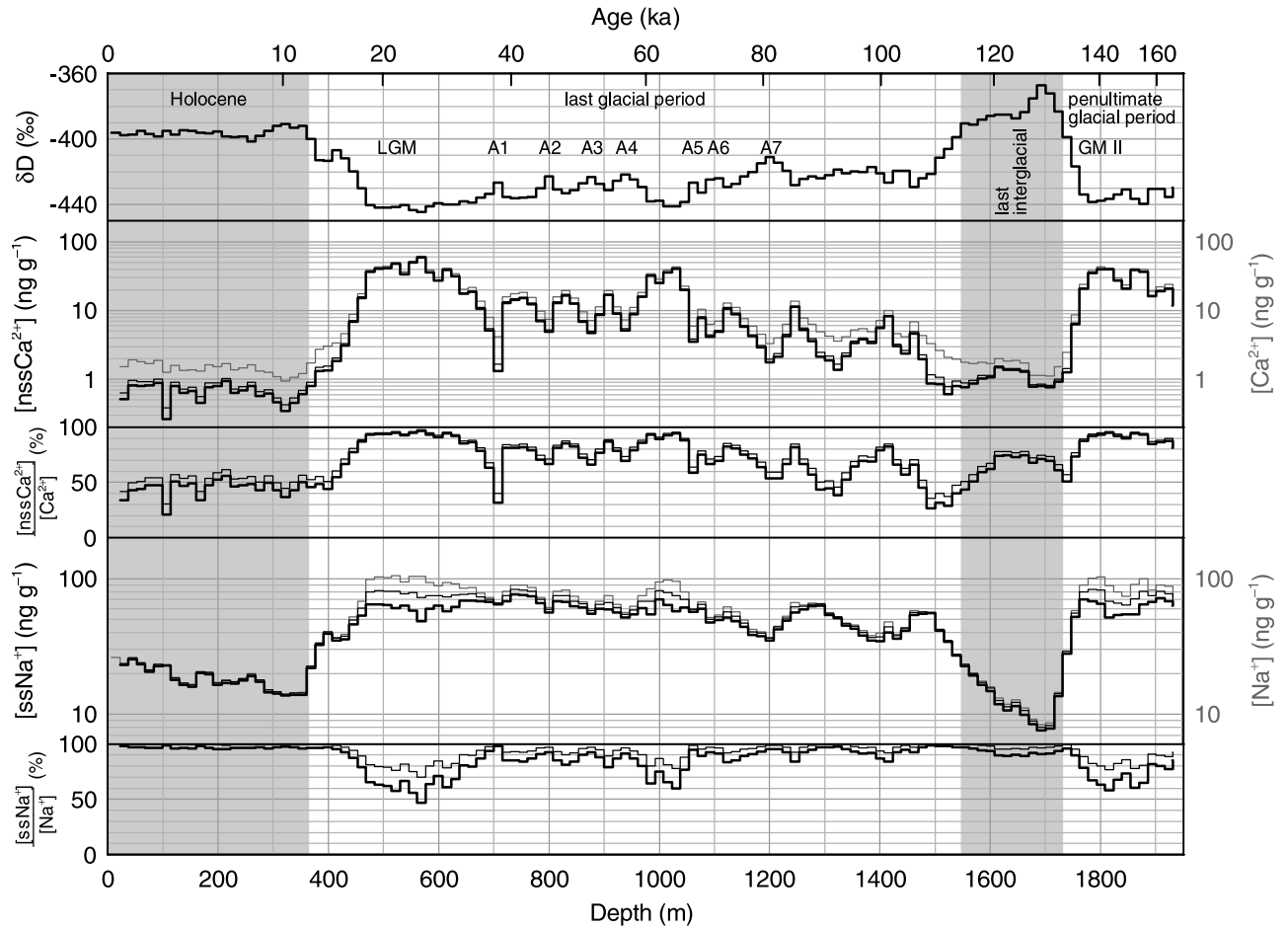

Figure 9. Calculated [ssNa$^+$] and [nssCa^{2+}] records (black lines), measured [Ca^{2+}] and [Na$^+$] data (gray lines), and resulting percentages of [ssNa$^+$]/[Na$^+$] and [nssCa^{2+}]/[Ca^{2+}] based on ion mass ratios derived in this study, shown along with δD [*EPICA community members*, 2004]. For comparison, [ssNa$^+$] and [nssCa^{2+}] calculated on the basis of literature values of $(Na/Ca)_{crust}$ and $(Na^+/Ca^{2+})_{ss}$ are shown as well (thin black lines). All data are averaged to 15.4 m mean values.

be compared with the situation encountered in the Antarctic realm, because they are crossing predominantly continental areas, as in the case of Arctic Haze, (sub)tropical ocean areas as in the case of Asian dust or subtropical to temperate seas as in the case of Saharan dust. The Antarctic situation stands out however, with transport over mainly cold water, being partly or substantially ice covered, and giving thus relatively little chance for intense updrafts en route. In summary, although Antarctica is much more isolated from dust sources than the Arctic, there is no reason to rule out that such episodes may have occurred, especially during glacial times.

4.5. Continental Versus Sea-Salt Aerosol Input Over the Last Glacial Cycle

[37] We calculated [ssNa$^+$], [nssCa^{2+}], [ssNa$^+$]/[Na$^+$], and [nssCa^{2+}]/[Ca^{2+}] on the basis of our new ion mass ratios and according to equations (3) and (4), assuming that the ion mass ratios are also valid for the late penultimate glacial period (Figure 9, showing 15.4 m mean values which correspond to approximately 500 a in the Holocene and 3000 a in the penultimate glacial period). Mean values for characteristic time intervals are summarized in Table 2. For comparison, the temperature proxy δD [*EPICA community members*, 2004], and [ssNa$^+$] and [nssCa^{2+}], both calculated using the literature value of $(Na/Ca)_{crust}$ (as used so far in glaciochemical studies) are shown as well.

[38] The main features of our new [nssCa^{2+}] record differ not much from previous ones (Figure 9). Less than half of the Holocene Ca^{2+} input in Dome C is shown to be of continental origin [see also *Röthlisberger et al.*, 2002], whereas it constitutes broadly two thirds in the last interglacial period (MIS 5e). During the glacial maxima (LGM and GM II of the penultimate glacial period) [nssCa^{2+}] accounts for more than 90% of the total [Ca^{2+}]. In the earlier part of the last glacial period, the percentage of [nssCa^{2+}] was highly variable, reaching the lowest levels during Antarctic warm events (e.g., A1–A7). Because of the strong dispersion of dust plumes during long-range transport from the southern South American source the results applies probably for most of the inland of the East Antarctic plateau [*Mulvaney et al.*, 2000].

[39] Looking at our [ssNa$^+$] record shows that in the Holocene nearly all and in MIS 5e still more than 90% of

Table 2. EPICA Dome C Mean Values and Percentages

Period[a]	Depth, m	$[Na^+]$, ng g^{-1}	$[ssNa^+]$, ng g^{-1}	$[ssNa^+]/[Na^+]$, %	$[Ca^{2+}]$, ng g^{-1}	$[nssCa^{2+}]$, ng g^{-1}	$[nssCa^{2+}]/[Ca^{2+}]$, %
Holocene	7–360	19	18	97	1.5	0.7	45
LGM	470–640	98	61	62	43	40	94
Last glacial	640–1470	64	55	88	12	9.5	72
MIS 5e	1550–1730	14	13	92	1.6	1.0	65
GM II	1760–1820	96	64	67	37	34	92

[a]LGM, last glacial maximum; MIS 5e, last interglacial; GM II, glacial maximum of the penultimate glacial period.

the total $[Na^+]$ originates from sea-salt aerosol input (Figure 9). However, during glacial maxima and around 60 ka, only around two thirds of the deposited Na^+ (LGM 47% to 71%) comes from the sea-salt source, whereas it is between 80% and 100% during remaining parts of the last glacial period. Especially under glacial conditions differences of our new $[ssNa^+]$ record compared to previous estimates are more pronounced than for $[nssCa^{2+}]$. The contribution of continental aerosol to the total Na^+ during cold glacial periods was larger than previously assumed, and using total Na^+ as a marine proxy [*Petit et al.*, 1999] overestimates the sea-salt input to central Antarctica during glacial times, as indicated already by *Delmas and Petit* [1994]. As sodium is often used to calculate enrichment factors in elemental compositions with respect to the marine source [e.g., *Tuncel et al.*, 1989] a higher continental contribution of halide aerosols on the East Antarctic plateau than previously assumed introduces larger uncertainties in the interpretation of such calculations.

[40] A more detailed discussion of these records with regard to southern high-latitude climate will be published by M. Bigler et al. (manuscript in preparation, 2006).

4.6. Preservation of the Seawater Ratio in the Aerosol During LGM

[41] Until now it was assumed that Cl^- had no significant continental source [*Röthlisberger et al.*, 2003]. Therefore it was argued that since the $[Cl^-]$ to $[Na^+]$ ratio during the LGM stayed close to the bulk seawater ratio, the continental contribution to the total Na^+ must be insignificant too. However, as for Na^+, we find a marine contribution to the total $[Cl^-]$ of only about 66% to 75% during LGM, and the continental ion mass ratio of $(Cl^-/Na^+)_{nss}$ between 0.9 and 1.8 is fairly close to $(Cl^-/Na^+)_{ss}$ between 1.8 and 2.0. Therefore the overall ratio of Cl^- to Na^+ around 1.7 [*Röthlisberger et al.*, 2003] during glacial maxima still corresponds to the bulk seawater ratio of $(Cl^-/Na^+)_{ss}$ = 1.8 despite the continental aerosol contribution.

5. Conclusions

[42] Thanks to the extremely high depth resolution of Ca^{2+} and Na^+ CFA data from the EPICA Dome C ice core we were able to derive for the first time directly mean ion mass ratios of the continental and the sea-salt aerosol deposited on the East Antarctic plateau. By inspecting ion mass ratios of exceptionally high Ca^+ and corresponding Na^+ peaks and vice versa we obtained the likely range of these ratios. Whereas most of the data show a mix of continental and sea-salt aerosol, we found a sufficient number of values that most likely represent a pure continental and a pure sea-salt aerosol input, respectively, allowing us to estimate a continental ion mass ratio $(Na^+/Ca^{2+})_{nss}$ of 0.94 ± 0.07 and a sea-salt ion mass ratio $(Na^+/Ca^{2+})_{ss}$ of 23 ± 1. Considering coarser resolved Cl^- data from the last glacial maximum, we further derived continental ion mass ratios with respect to Cl^- and found $(Cl^-/Ca^{2+})_{nss}$ to be in the range from 0.8 to 1.7 and $(Cl^-/Na^+)_{nss}$ in the range 0.9 to 1.8.

[43] All continental ion mass ratios are distinctly higher than previously assumed pointing to a higher continental contribution to Na^+ and Cl^- from the restricted source area of southern South America especially during glacial periods. Indeed, halide soils and halide continental aerosols are reported from the expected source region and the latter are found also in midlatitude continental ice cores. However, a contribution of marine clays originating directly or indirectly from exposed continental shelf areas cannot be ruled out. Elemental ratios of mean crust that have been used up to now for source contribution estimates turn out to be unsuitable with regard to the aerosol properties recorded in East Antarctic ice cores. Furthermore, the application of total sodium as a marine reference to calculate enrichment factors is inappropriate for East Antarctic ice core samples from cold glacial periods. On the other hand, the apparent preservation of the bulk seawater ratio (Cl^-/Na^+) during the LGM at Dome C despite the considerable continental contribution is explained by the continental ion mass ratio $(Cl^-/Na^+)_{nss}$ being quite close to the bulk seawater ratio.

[44] The deduced sea-salt ion mass ratio $(Na^+/Ca^{2+})_{ss}$ of 23 ± 1 is within the range of values given by the ion mass ratio in bulk seawater of 26 and by the ion mass ratio of brine-derived sea-salt aerosol of 23. Further work is needed to pin down the relative contributions of these two sea-salt aerosol sources around Antarctica to the East Antarctic plateau, especially during glacial periods.

[45] Our refined $[nssCa^{2+}]$ record, as assumed to be a pure continental proxy, does not differ very much from previous results and interpretations. On the other hand, $[ssNa^+]$ shows differences, mainly during cold glacial periods. On average, more than one third of the entire water-soluble $[Na^+]$ originates from continental aerosols. Hence $[Na^+]$ records from the East Antarctic plateau do not represent a pure marine signal during glacial times. Our $[nssCa^{2+}]$ and $[ssNa^+]$ records are discussed with regard to the climate of the southern South Hemisphere by M. Bigler et al. (manuscript in preparation, 2006).

[46] Similar estimates should be done on ice core sections from other Antarctic sites in order to corroborate our findings. This approach might also allow the characterization of

differences in dust source regions for different Antarctic sites, if existent. However, such an analysis requires high-resolution data that are not yet available from other ice cores. Upcoming results from the second deep drilling in the frame of EPICA performed in Dronning Maud land in the Atlantic sector of East Antarctica offer the possibility to substantiate our findings.

[47] **Acknowledgments.** This work is a contribution to the "European Project for Ice Coring in Antarctica" (EPICA), a joint European Science Foundation (ESF)–EC scientific program, funded by the European Commission and by national contributions from Belgium, Denmark, France, Germany, Italy, the Netherlands, Norway, Sweden, Switzerland, and the United Kingdom. This is EPICA publication 136. We thank all the persons involved in the fieldwork to obtain this comprehensive data set, Sune Olander Rasmussen for the deconvolution calculations, and Eric W. Wolff and the two anonymous reviewers for helpful comments. M.B. thanks the Swiss National Science Foundation (SNF) for financial support.

References

Barnes, P. R. F., E. W. Wolff, H. M. Mader, R. Udisti, E. Castellano, and R. Röthlisberger (2003), Evolution of chemical peak shapes in the Dome C, Antarctica, ice core, *J. Geophys. Res.*, *108*(D3), 4126, doi:10.1029/2002JD002538.

Basile, I., F. E. Grousset, M. Revel, J. R. Petit, P. E. Biscaye, and N. I. Barkov (1997), Patagonian origin of glacial dust deposited in East Antarctica (Vostok and Dome C) during glacial stages 2, 4 and 6, *Earth Planet. Sci. Lett.*, *146*(3–4), 573–589.

Blunier, T., and E. J. Brook (2001), Timing of millennial-scale climate change in Antarctica and Greenland during the last glacial period, *Science*, *291*, 109–112.

Bory, A. J.-M., P. E. Biscaye, and F. E. Grousset (2003), Two distinct seasonal Asian source regions for mineral dust deposited in Greenland (NorthGRIP), *Geophys. Res. Lett.*, *30*(4), 1167, doi:10.1029/2002GL016446.

Bouza, P., H. F. Delvalle, and P. A. Imbellone (1993), Micromorphological, physical, and chemical characteristics of soil crust types of the central Patagonia region, Argentina, *Arid Soil Res. Rehabil.*, *7*(4), 355–368.

Bowen, H. J. M. (1979), *Environmental Chemistry of the Elements*, Elsevier, New York.

Correia, A., R. Freydier, R. J. Delmas, J. C. Simoes, J. D. Taupin, B. Dupre, and P. Artaxo (2003), Trace elements in South America aerosol during 20th century inferred from a Nevado Illimani ice core, eastern Bolivian Andes (6350m asl), *Atmos. Chem. Phys.*, *3*, 1337–1352.

de Angelis, M., N. I. Barkov, and V. N. Petrov (1987), Aerosol concentrations over the last climatic cycle (160 kyr) from an Antarctic ice core, *Nature*, *325*(6102), 318–321.

de Angelis, M., N. I. Barkov, and V. N. Petrov (1992), Sources of continental dust over Antarctica during the last glacial cycle, *J. Atmos. Chem.*, *14*, 233–244.

Delmas, R. J., and J. R. Petit (1994), Present Antarctic aerosol composition: A memory of ice age atmospheric dust?, *Geophys. Res. Lett.*, *21*(10), 879–882.

Delmonte, B., I. Basile-Doelsch, J.-R. Petit, V. Maggi, M. Revel-Rolland, A. Michard, E. Jagoutz, and F. Grousset (2004), Comparing the EPICA and Vostok dust records during the last 220,000 years: Stratigraphical correlation and provenance in glacial periods, *Earth Sci. Rev.*, *66*, 63–87.

EPICA community members (2004), Eight glacial cycles from an Antarctic ice core, *Nature*, *429*(6992), 623–628.

Fischer, H., F. Traufetter, H. Oerter, R. Weller, and H. Miller (2004), Prevalence of the Antarctic Circumpolar Wave over the last two millenia recorded in Dronning Maud Land ice, *Geophys. Res. Lett.*, *31*, L08202, doi:10.1029/2003GL019186.

Gersonde, R., X. Crosta, A. Abelmann, and L. Armand (2005), Sea-surface temperature and sea ice distribution of the Southern Ocean at the EPILOG last glacial maximum: A circum-Antarctic view based on siliceous microfossil records, *Quat. Sci. Rev.*, *24*(7–9), 869–896.

Ghermandi, G., R. Cecchi, M. Capotosto, and F. Marino (2003), Elemental composition determined by PIXE analysis of the insoluble aerosol particles in EPICA-Dome C ice core samples representing the last 27000 years, *Geophys. Res. Lett.*, *30*(22), 2176, doi:10.1029/2003GL018169.

Göktas, F., H. Fischer, H. Oerter, R. Weller, S. Sommer, and H. Miller (2002), A glacio-chemical characterization of the new EPICA deep-drilling site on Amundsenisen, Dronning Maud Land, Antarctica, *Ann. Glaciol.*, *35*, 347–354.

Grousset, F. E., P. E. Biscaye, M. Revel, J. R. Petit, K. Pye, S. Joussaume, and J. Jouzel (1992), Antarctic (Dome C) ice-core dust at 18 ky BP: Isotopic constraints on origins, *Earth Planet. Sci. Lett.*, *111*(1), 175–182.

Guilderson, T. P., L. Burckle, S. Hemming, and W. R. Peltier (2000), Late Pleistocene sea level variations derived from the Argentine Shelf, *Geochem. Geophys. Geosyst.*, *1*(12), doi:10.1029/2000GC000098.

Hara, K., K. Osada, M. Kido, M. Hayashi, K. Matsunaga, Y. Iwasaka, T. Yamanouchi, G. Hashida, and T. Fukatsu (2004), Chemistry of sea-salt particles and inorganic halogen species in Antarctic regions: Compositional differences between coastal and inland stations, *J. Geophys. Res.*, *109*, D20208, doi:10.1029/2004JD004713.

Harrison, S. P., K. E. Kohfeld, C. Roelandt, and T. Claquin (2001), The role of dust in climate changes today, at the last glacial maximum and in the future, *Earth Sci. Rev.*, *54*(1–3), 43–80.

Holland, H. D. (1978), *Chemistry of the Atmosphere and Oceans*, John Wiley, Hoboken, N. J.

Huybrechts, P., and C. Zweck (2006), Cryosphere, in *Encyclopedia of Paleoclimatology and Ancient Environments*, edited by V. Gornitz, Springer, New York, in press.

Iriondo, M. (2000), Patagonian dust in Antarctica, *Quat. Int.*, *68*, 83–86.

Kreutz, K. J., V. B. Aizen, L. D. Cecil, and C. P. Wake (2001), Oxygen isotopic and soluble ionic composition of a shallow firn core, Inilchek glacier, central Tien Shan, *J. Glaciol.*, *47*(159), 548–554.

Krinner, G., and C. Genthon (2003), Tropospheric transport of continental tracers towards Antarctica under varying climatic conditions, *Tellus, Ser. B*, *55*(1), 54–70.

Legrand, M., and P. Mayewski (1997), Glaciochemistry of polar ice cores: A review, *Rev. Geophys.*, *35*(3), 219–243.

Legrand, M. R., C. Lorius, N. I. Barkov, and V. N. Petrov (1988), Vostok (Antarctica) ice core: Atmospheric chemistry changes over the last climatic cycle (160,000 years), *Atmos. Environ.*, *22*(2), 317–331.

Legrand, M., S. Preunkert, D. Wagenbach, and H. Fischer (2002), Seasonally resolved Alpine and Greenland ice core records of anthropogenic HCl emissions over the 20th century, *J. Geophys. Res.*, *107*(D12), 4139, doi:10.1029/2001JD001165.

Leinen, M., and M. Sarnthein (Eds.) (1987), *Paleoclimatology and Paleometerology: Modern and Past Patterns of Global Atmospheric Transport*, *NATO ASI Ser., Ser. C*, vol. 282, Springer, New York.

Littot, G. C., R. Mulvaney, R. Röthlisberger, R. Udisti, E. W. Wolff, E. Castellano, M. de Angelis, M. E. Hansson, S. Sommer, and J. P. Steffensen (2002), Comparison of analytical methods used for measuring major ions in the EPICA Dome C (Antarctica) ice core, *Ann. Glaciol.*, *35*, 299–305.

Lunt, D. J., and P. J. Valdes (2001), Dust transport to Dome C, Antarctica at the last glacial maximum and present day, *Geophys. Res. Lett.*, *28*(2), 295–298.

Mulvaney, R., R. Röthlisberger, E. W. Wolff, S. Sommer, J. Schwander, M. A. Hutterli, and J. Jouzel (2000), The transition from the last glacial period in inland and near-coastal Antarctica, *Geophys. Res. Lett.*, *27*(17), 2673–2676.

Ohno, H., M. Igarashi, and T. Hondoh (2005), Salt inclusions in polar ice core: Location and chemical form of water-soluble impurities, *Earth Planet. Sci. Lett.*, *232*(1–2), 171–178.

Olivier, S., et al. (2003), Glaciochemical investigation of an ice core from Belukha glacier, Siberian Altai, *Geophys. Res. Lett.*, *30*(19), 2019, doi:10.1029/2003GL018290.

Petit, J. R., et al. (1999), Climate and atmospheric history of the past 420,000 years from the Vostok ice core, Antarctica, *Nature*, *399*, 429–436.

Prospero, J. M., P. Ginoux, O. Torres, S. E. Nicholson, and T. E. Gill (2002), Environmental characterization of global sources of atmospheric soil dust identified with the Nimbus 7 Total Ozone Mapping Spectrometer (TOMS) absorbing aerosol product, *Rev. Geophys.*, *40*(1), 1002, doi:10.1029/2000RG000095.

Ramsperger, B., L. Herrmann, and K. Stahr (1998a), Dust characteristics and source-sink relations in eastern west Africa (SW-Niger and Benin) and South America (Argentinean pampas), *Z. Pflanzenern. Bodenkunde*, *161*(4), 357–363.

Ramsperger, B., N. Peinemann, and K. Stahr (1998b), Deposition rates and characteristics of aeolian dust in the semi-arid and sub-humid regions of the Argentinean Pampa, *J. Arid Environ.*, *39*(3), 467–476.

Rasmussen, S. O., K. K. Andersen, S. J. Johnsen, M. Bigler, and T. McCormack (2005), Deconvolution-based resolution enhancement of chemical ice core records obtained by continuous flow analysis, *J. Geophys. Res.*, *110*, D17304, doi:10.1029/2004JD005717.

Röthlisberger, R., M. Bigler, M. Hutterli, S. Sommer, B. Stauffer, H. G. Junghans, and D. Wagenbach (2000), Technique for continuous high-resolution analysis of trace substances in firn and ice cores, *Environ. Sci. Technol.*, *34*(2), 338–342.

Röthlisberger, R., R. Mulvaney, E. W. Wolff, M. A. Hutterli, M. Bigler, S. Sommer, and J. Jouzel (2002), Dust and sea salt variability in central

East Antarctica (Dome C) over the last 45 kyrs and its implications for southern high-latitude climate, *Geophys. Res. Lett.*, *29*(20), 1963, doi:10.1029/2002GL015186.

Röthlisberger, R., R. Mulvaney, E. W. Wolff, M. A. Hutterli, M. Bigler, M. de Angelis, M. E. Hansson, J. P. Steffensen, and R. Udisti (2003), Limited dechlorination of sea-salt aerosols during the last glacial period: Evidence from the European Project for Ice Coring in Antarctica (EPICA) Dome C ice core, *J. Geophys. Res.*, *108*(D16), 4526, doi:10.1029/2003JD003604.

Röthlisberger, R., M. Bigler, E. W. Wolff, F. Joos, E. Monnin, and M. A. Hutterli (2004), Ice core evidence for the extent of past atmospheric CO_2 change due to iron fertilisation, *Geophys. Res. Lett.*, *31*, L16207, doi:10.1029/2004GL020338.

Schwander, J., J. Jouzel, C. U. Hammer, J.-R. Petit, R. Udisti, and E. Wolff (2001), A tentative chronology for the EPICA Dome Concordia ice core, *Geophys. Res. Lett.*, *28*(22), 4243–4246.

Smith, J., D. Vance, R. A. Kemp, C. Archer, P. Toms, M. King, and M. Zárate (2003), Isotopic constraints on the source of Argentinian loess: With implications for atmospheric circulation and the provenance of Antarctic dust during recent glacial maxima, *Earth Planet. Sci. Lett.*, *212*(1–2), 181–196.

Sommer, S., D. Wagenbach, R. Mulvaney, and H. Fischer (2000), Glaciochemical study spanning the past 2 kyr on three ice cores from Dronning Maud Land, Antarctica: 2. Seasonally resolved chemical records, *J. Geophys. Res.*, *105*(D24), 29,423–29,433.

Sun, J. (2002), Provenance of loess material and formation of loess deposits on the Chinese Loess Plateau, *Earth Planet. Sci. Lett.*, *203*(3–4), 845–859.

Tuncel, G., N. K. Aras, and W. H. Zoller (1989), Temporal variations and sources of elements in the South Pole atmosphere: 1. Nonenriched and moderately enriched elements, *J. Geophys. Res.*, *94*(D10), 13,025–13,038.

Wagenbach, D., F. Ducroz, R. Mulvaney, L. Keck, A. Minikin, M. Legrand, J. S. Hall, and E. W. Wolff (1998), Sea-salt aerosol in coastal Antarctic regions, *J. Geophys. Res.*, *103*(D9), 10,961–10,974.

Wake, C. P., P. A. Mayewski, Z. C. Xie, P. Wang, and Z. Q. Li (1993), Regional distribution of monsoon and desert dust signals recorded in Asian glaciers, *Geophys. Res. Lett.*, *20*(14), 1411–1414.

Warneck, P. (1999), *Chemistry of the Natural Atmosphere*, 927 pp., Elsevier, New York.

Wolff, E. W., A. M. Rankin, and R. Röthlisberger (2003), An ice core indicator of Antarctic sea ice production?, *Geophys. Res. Lett.*, *30*(22), 2158, doi:10.1029/2003GL018454.

Zárate, M. A. (2003), Loess of southern South America, *Quat. Sci. Rev.*, *22*(18–19), 1987–2006.

M. Bigler, Ice and Climate Research, Niels Bohr Institute, University of Copenhagen, Juliane Maries Vej 30, Copenhagen DK-2100, Denmark. (bigler@gfy.ku.dk)

F. Lambert and T. F. Stocker, Climate and Environmental Physics, Physics Institute, University of Bern, Sidlerstrasse 5, CH-3012 Bern, Switzerland.

R. Röthlisberger, British Antarctic Survey, High Cross, Madingley Road, Cambridge CB3 0ET, UK.

D. Wagenbach, Institut für Umweltphysik, University of Heidelberg, Im Neuenheimer Feld 229, D-69120 Heidelberg, Germany.